Chapter 20

EVIDENCES OF NEW BIOPHYSICAL PROPERTIES OF MICROTUBULES

Rita Pizzi[1], Giuliano Strini[2], Silvia Fiorentini[1], Valeria Pappalardo[3] and Massimo Pregnolato[3]

[1]Dipartimento di Tecnologie dell'Informazione - Via Bramante 65, Università degli Studi di Milano, 26013 Crema - Italy
[2]Dipartimento di Fisica – Via Celoria 16, Università degli Studi di Milano, 20133 Milano - Italy
[3]QuantumBiolab- Dipartimento di Chimica Farmaceutica – Viale Taramelli 12, Università degli Studi di Pavia, 27100 Pavia - Italy.

ABSTRACT

Microtubules (MTs) are cylindrical polymers of the protein tubulin, are key constituents of all eukaryotic cells cytoskeleton and are involved in key cellular functions. Among them MTs are claimed to be involved as sub-cellular information or quantum information communication systems. MTs are the closest biological equivalent to the well known carbon nanotubes (CNTs) material. We evaluated some biophysical properties of MTs through two specific physical measures of resonance and birefringence, on the assumption that when tubulin and MTs show different biophysical behaviours, this should be due to the special structural properties of MTs. The MTs, as well as CNTs, may behave as oscillators, this could make them superreactive receivers able to amplify radio wave signals. Our experimental approach verified the existence of mechanical resonance in MTs at a frequency of 1510 MHz. The analysis of the results of birefringence experiment highlights that the MTs react to electromagnetic fields in a different way than tubulin.

INTRODUCTION

Microtubules (MTs) are cylindrical protein polymers and are key constituents of all eukaryotic cells cytoskeleton. They are involved in the regulation of essential cellular functions such as the transport of materials within the cell, the movement of cytoplasmic organelles or vesicles and the cell division [1]. These filaments are constructed from αβ-tubulin heterodimers that through a process of polymerization and depolymerization will arrange to form a slightly distorted hexagonal lattice. This dynamic nature makes MTs sensitive to several pharmacological agents, i.e. some classes of anticancer agents that are able to destroy or stabilize their structure.

Several MTs biophysical characteristics have been studied in the last decade and are increasing mainly due to the close analogy that exists between MTs and carbon nanotubes (CNTs).

CNTs display a wide range of physical effects among them electronic properties are particularly attractive. In the case of MTs suitable experiments are more difficult to be performed and required expertises in both biological and physical disciplines.

The purpose of this research project is the study and evaluation of some biophysical properties of MTs through two specific physical measures of birefringence and resonance, on the assumption that when tubulin and MTs show different biophysical behaviours, this should be due to the special structural properties of MTs.

Tubulins and Microtubules

MTs are stiff cytoskeletal filaments characterized by a tubelike structure, they are also relatively fragile and more liable to break than microfilaments or intermediate-filaments. The building block of a MT is a 110-kDa heterodimeric protein said tubulin, that is the association product of two different subunits, designated α and β tubulin [2,3] and encoded by separate genes. The word tubulin always refers to the αβ heterodimer, that is usually considered as one unit, although the association is only due to non-covalent interactions. Each monomer of α and β tubulin is a compact ellipsoid of approximate dimensions 46 x 40 x 65 A° (width, height, and depth, respectively); while dimensions of αβ-heterodimer are 46 x 80 x 65 A°. Both α- and β- tubulin is composed of approximately 450 amino acids and, in spite of their sequence identity (approximately 40%), slight folding difference can be seen. The two tubulins exhibit homology with a 40,000-MW bacterial GTPase, called FtsZ, a ubiquitous protein in eubacteria and archeobacteria. Like tubulin, this bacterial protein has the ability to polymerize and participates in cell division. Perhaps the protein carrying out these ancestral functions in bacteria was modified in the course of evolution to fulfill the diverse roles of MTs in eukaryotes [4].

While many questions remain about tubulin, in 1998 Nogales et al. obtained the structure of the αβ-heterodimer at 3,7 Å resolution by electron crystallography of zinc-induced crystalline sheets of tubulin stabilized with taxol [5]. In 2001 this structures has been refined [6]. The core of each monomer contains two β-sheets of 6 and 4 strands, that are surrounded by α-helices, and a pair of globular domains set on either side of a central (core) helix H7. The monomer is a very compact structure and can be divided into three functional and

sequential domains. The larger globular domain comprises the N-terminal half of the polypeptide that include the binding site for the guanosine nucleotide. The second globular domain has a binding site for Taxol on the opposite side from its contact with the nucleotide base and a predominantly helical carboxy-terminal region which probably constitutes the binding surface for motor proteins.

Calculations of the potential energy displayed that tubulin is quite highly negatively charged at physiological pH and that much of the charge is concentrated on the C-terminus of each tubulin monomer. The C-terminal end forms two long helices (H11 and H12) connected by a U-turn while the final 13 residues of α-tubulin and 9 residues of β-tubulin are too disordered in the 2D crystals to show up as electron density but are assumed to project out into the solution [7]. A detailed map of the electric charge distribution on the surface of the tubulin dimer showed that the C-termini, which extend outward, carry a significant electric charge [8]. In physiological conditions (neutral pH), the negative charge of the carboxy-terminal region causes it to remain extended due to the electrostatic repulsion within the tail. Under more acidic conditions, the negative charge of this region is reduced by association of hydrogen ions. The effect is to allow these tails to acquire a more compact form by folding.

Each tubulin heterodimers binds two molecules of guanine nucleoside phosphates (GTP) and exhibits GTPase activity that is closely linked to assembly and disassembly of MTs. One GTP-binding site is located in α-tubulin at the interfaces between α- and β- tubulin monomers; in this site GTP is trapped irreversibly and it is not hydrolyzable. The second site is located at the surface of the β-tubulin subunit; in this site GTP is bound reversibly and it is freely hydrolyzable to GDP. The GTP bound to β-tubulin modulates the addition of other tubulin subunits at the ends of the MT.

Recently important information about tubulin conformational changes during the MTs polymerization have been obtained through X-ray crystallography [9].

The general structure of MTs has been established experimentally [10,11]. MTs have been considered as helical polymers and they are built by the self-association of the αβ-heterodimer. In those polymers tubulin subunits are arranged in a hexagonal lattice which is slightly twisted, resulting in different neighboring interactions among each subunit. The polymerization occurs in a two-dimensional process that involves two types of contacts between tubulin subunits. The first process involve head-to-tail binding of heterodimers and it results in polar protofilaments that run along the length of the MT. The second process involve lateral interactions between parallel protofilaments and it complete the MT wall to form a hollow tube [12]. The longitudinal contacts along protofilaments appear to be much stronger than those between adjacent protofilaments [13].

The head-to-tail arrangement of the α- and β-tubulin dimers in a protofilament confers an overall polarity on a MT. All protofilaments in a MT have the same orientation. One end of a MT is ringed by α-tubulin and it is designed minus end because here the GTP is not exchangeable. The opposite end is ringed by β-tubulin, it is designed plus end because here the nucleotide is exchangeable. The longitudinal interactions between tubulin subunits in the protofilament seem to involve exclusively heterologous (α-β) subunits. In contrast, the lateral interactions involve predominantly homologous subunits (α-α, β-β) but heterologous interactions (α-β) occur also. When all or most lateral interactions are α-β the lattice is known as the A-lattice; instead, when all lateral contacts are α-α or β-β the lattice is known as the B-lattice.

Assembly mechanism of α- and β- tubulin gives rise *in vitro* to a variety of cylindrical structures that differ by their protofilament and monomer helix-start numbers [14-19]. In contrast, most MTs assembled *in vivo* seem to be composed of 13 protofilaments, although many exceptions have been noted in different species and cell types; for example in neurons of the nematode *Caenorhabditis elegans* some specialized MTs have 15-protofilaments [20,21]. The lengths of MTs vary but commonly reach 5-10 µm dimensions; and their diameter depends on the protofilament number. For example in the case of 13 protofilaments the tube has an outer diameter of 23 nm and an inner diameter of roughly 15 nm.

Microtubules Quantum Theories

In the last decade many theories and papers have been published concerning the biophysical properties of MTs including the hypothesis of MTs implication in coherent quantum states in the brain evolving in some form of energy and information transfer.

The most discussed theory on quantum effects involving MTs has been proposed by Hameroff and Penrose that published the OrchOR Model in 1996 [22,23].

They supposed that quantum-superposed states develop in tubulins, remain coherent and recruit more superposed tubulins until a mass-time-energy threshold, related to quantum gravity, is reached (up to 500 msec). This model has been discussed and refined for more than 10 years, mainly focusing attention to the decoherence criterion after the Tegmark critical paper of 2000 [24, 25] and proposing several methods of shielding MTs against the environment of the brain [26-28]. In the Hameroff model MTs perform a kind of quantum computation through the tubulins working like a cellular automata. The MTs interior works as an electromagnetic wave guide, filled with water in an organized collective states, transmitting information through the brain [29].

In the same years Nanopoulos et al adopted the string theory to develop a so called QED-Cavity model predicting dissipationless energy transfer along MTs as well as quantum teleportation of states at near room temperature [30-33].

The Tuszynski approach is based on the biophysical aspects of MTs. Tubulins have electric dipole moments due to asymmetric charges distribution and MTs can be modeled as a lattice of orientated dipoles that can be in random phase, ferroelectric (parallel-aligned) and an intermediate weakly ferroelectric phase like a spin-glass phase [34-36]. The model has been sustained by Faber et al [37] who considered a MT as a classical subneuronal information processor.

In 1994 Jibu and Yasue suggested that the Fröhlich dynamics of ordered water molecules and the quantized electromagnetic field confined inside the hollow MTs core can give rise to the collective quantum optical modes responsible for the phenomenon of superradiance by which any incoherent molecular electromagnetic energy can be transformed in a coherent photon inside the MTs. These photons propagate along the internal hollow core as if the optical medium were transparent and this quantum theoretical phenomenon is called "self-induced transparency".

A decade before, applying quantum field theory (QFT), Del Giudice et al [38,39] reported that electromagnetic energy penetrating into cytoplasm would self-focus inside

filaments whose diameter depend on symmetry breaking (Bose condensation) of ordered water dipoles. The diameter calculated was exactly the inner diameter of MTs (15 nm).

In any case, all phenomena occurring within the brain, both at macroscopic or microscopic level, can be related to some form of phase transition and a number of authors [40,41] pointed out the inconsistence of a quantum mechanical framework based only on traditional computational schemata. It is to be recalled, in this regard, that these schemata have been introduced to deal with particles, atoms, or molecules, and are unsuitable when applied to biological phenomena. In particular Pessa suggested that adopting a wider framework of QFT and, in particular, the dissipative version of it, relying on the doubling mechanism, we could achieve a generalization of QFT able to account for change phenomena in the biological world [42-44].

Carbon Nanotubes and Microtubules

The time required to process and transfer information faster has reached the point at which quantum effects can no longer be neglected. The electronics industry will evolve from the technology based on silicon towards innovative materials with new physical properties. These new materials include the carbon nanotubes which currently represent one of the most promising alternatives to overcome the current limits of silicon.

Currently, with a large commitment of academic and industrial scientists, the research is developing nanotubes with extremely advanced and useful properties, as they can act both as semiconductors and as superconductors. Thanks to the structure of these nanoscale materials, their properties are not restricted to classical physics, but presents a wide range of quantum mechanical effects. These may lead to an even more efficient tool for information transfer.

Quantum transport properties of CNTs has been reviewed by Roche et al [45] both from a theoretical and experimental view. Recently has been described the low-temperature spin relaxation time measurement in a fully tunable CNT double quantum dots. This is an interesting study for new microwave-based quantum information processing experiments with CNTs [46].

According to Pampaloni et al. [47] CNTs are the closest equivalent to MTs among the known nanomaterials. Although their elastic moduli are different, MTs and CNTs have similar mechanical behaviours. They are both exceptionally resilient and form large boundless with improved stiffness. Nanobiotechnology can move towards a next generation of materials with a wide range of functional properties. As suggest by Michette et al, MTs associated with carbon chemistry will allow to build complex macromolecular assemblies for sharing the exciting electronic properties of semi- and super-conductors [48].

Resonance Experiment on Microtubules

Antennas are devices capable to transform an electromagnetic field into an electrical signal, or to radiate, in the form of electromagnetic field, the electrical signal they are fed by. When powered by an electrical signal to their ends, antennas absorb energy and return it in the surrounding space as electromagnetic waves (transmitting antenna), or absorb energy

from an electromagnetic wave and generate a voltage to their ends (receiving antenna). On theoretical bases any conductive object acts as an antenna, regardless of the electromagnetic wave frequency they are hit or the signal that is fed by. In particular, any tubular conductor cable, resonating mechanically, acts as a cavity antenna. The magnitude of the effect becomes significant when the frequency corresponds to the resonance frequency and in this case the output voltage can be used for receiving and transmitting radio waves. The resonance is a physical condition that occurs when a damped oscillating system is subjected to a periodic solicitation with a frequency equal to the system oscillation. A resonance phenomenon causes a significant increase in the extent of the oscillations that corresponds to a remarkable accumulation of energy within the oscillator.

Recent observations and experiments on CNTs have led to the development of an array of CNTs able to act as antennas [49]. These, instead to transmit and receive radio waves (measured in meters), due to their scale capture wavelengths at the nanoscale (measured in nanometers). In the study of the physical properties of MTs compared with those of CNTs, it is desired to search and analyze a possible reaction to microwaves, observing any ability of MTs to absorb or emit like antennas. The MTs, as well as CNTs, may behave as oscillators, this could make them superreactive receivers able to amplify the signals.

Our experimental approach was intended to verify the existence of mechanical resonance in MTs, in analogy with the CNTs, at the frequency that amplifies the wave.

Birefringence Experiment on Microtubules

Birefringence is an optical property of materials that arises from the interaction of light with oriented molecular and structural components [50]. Birefringence is the decomposition of a beam of light into two rays that occurs when the light crosses specific anisotropic media depending on the polarization of the light. The interaction between light and magnetic field in a medium results in the rotation of the plane of polarization proportional to the intensity of the magnetic field component in the direction of the beam of light (Faraday effect). By means of a polarized light and a suitable detection apparatus, it is possible to observe the associated birefringence and, therefore, the index of orientation of MTs subjected either to transverse electric fields and to transverse and longitudinal magnetic fields [51].

We performed *in vitro* experiment on different samples of MTs and tubulins, in stabilizing buffer solution, and measured the polarization under controlled conditions in order to determine different effects in the interaction of almost static electromagnetic fields. For our comparative experiments the variation of the refraction index is important because it is a function of the wavelength of the electromagnetic radiation and the nature of the crossed material.

Behavioural differences observed between samples of tubulin and MTs, would lead us to understand weather the cavity structure in the MT reacts in a peculiar way in response to specific stimuli or not.

MATERIALS AND METHODS

Materials

Stabilized microtubules (MTs, #MT001-A), tubulin (#TL238), taxol (# TXD01), GTP (#BST06) and General Tubulin Buffer (# BST01) are supplied by Cytoskeleton Inc. Denver, CO. USA.

Preparation of buffer MT: MTs resuspension buffer is obtained by adding 100 µl of 2mM taxol stock in dry DMSO to 10 ml of room temperature PM buffer (15 mM PIPES pH 7.0, 1 mM MgCl2). It is important to make sure that PM buffer is at room temperature as taxol will precipitate out of solution if added to cold buffer. Resuspended taxol should be stored at -20 °C.

Preparation of buffer T: GTP stock solution (100mM) is added to General Tubulin Buffer (80 mM PIPES pH 6.9, 2 mM MgCl2, 0.5 mM EGTA) at a final concentration of 1mM GTP. The buffer T will be stable for 2-4 hours on ice.

Microtubules Reconstitution. 1 ml of buffer MT is added to 1 mg of lyophilized MTs and mixed gently. Resuspended MTs are left at room temperature for 10–15 minutes with occasional gentle mixing. The MTs are now ready to use. They are at a mean length of 2 µm and the tubulin concentration is 1mg/ml. MTs will be stable for 2-3 days at room temperature, although it should be noted that the mean length distribution will increase over time. MTs can be snap frozen in liquid nitrogen and stored at -70 °C.

Tubulin Reconstitution. 1 mg of lyophilized tubulin is resuspended in 1 ml of buffer T at 0-4 °C (final tubulin concentration is 1 mg/ml). The reconstituted tubulin solution is not stable and needs to be used soon after its preparation.

Microwave Generator. The bench for the MTs resonance experiment consisted of two ¼ wave dipole custom antennas centered on a frequency of 1.5 GHz. The antennas have been placed on the same horizontal plane and spaced 1.6 in. The test-tube containing the solution was placed between the antennas. The system was placed in a Mu-metal container in order to shield the measurement system from any external signal. The first antenna was connected with a shielded cable to a Polarad mod. 1105 Microwave Signal Generator (Figure 1), generating frequencies between 0.8 GHz and 2.5 GHz. The second antenna shielded cable was connected with an Avantest mod. TR4131 Spectrum Analyzer. The experiment displays changes in the resonance reference peak of the tested material. If the peak is lower the analyzed sample is absorbing, if higher it is emitting electromagnetic energy.

Polarimeter specifications. For the measurement a polarimeter was prepared. In a classic polarimeter a monochromatic source radiates a beam of light (initially not polarized) that is sent on a pair of polarized filters (normally Nicol prisms) oriented so as to polarize light. In the following, the beam of polarized light crosses a cuvette containing the test solution which, if optically active, rotates both polarization planes of light. Finally, the beam passes through a

polarized filter, the analyzer, whose main section is rotatable. A more descriptive schema is depicted in the following (Figure 2).

The light source consists of a Hughes 3222HP Helium-Neon Laser, 633 nm, power 5 mW. The magnetic field is 18 Gauss RMS for the 632 Hz test cuvette and 9.8 Gauss RMS for the 610.1 Hz cuvette, while the applied electric field (632 Hz) is 1 Volt/cm RMS.
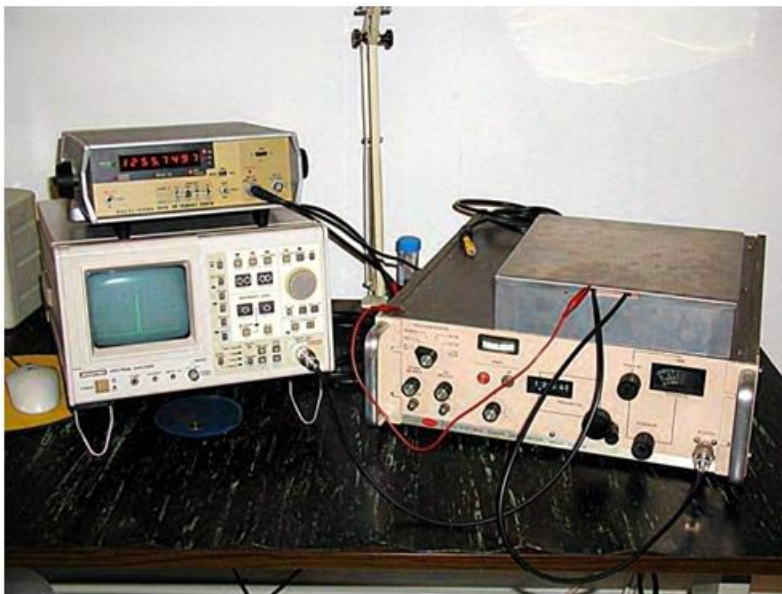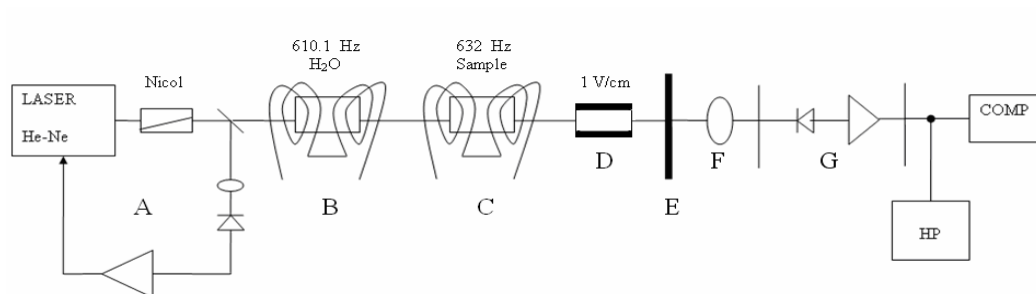

Figure 1. Microwave Signal Generator

Figure 2. Scheme of the polarimeter
A: Elio-Neon Laser (Hughes 3222H-P, 633 nm; 5 mW max; Polarizing Nicol; beam splitter
B : cuvette and 610.1 Hz coil for the reference cell
C: cuvetta and 632 Hz coil for the sample
D: electric field cell
E: analyzer filter
F: lens that focuses the beam on the photodiode
G: photodiode and amplifier
HP : spectrum analyzer (HP 3582A) for on-line check
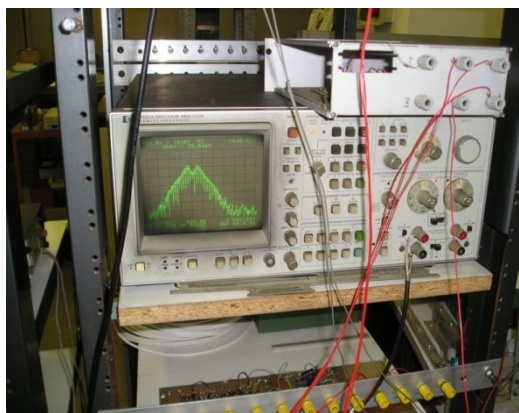COMP : data acquisition system

Figure 3. Spectrum analyzer HP 3582A

The cuvettes used for the magnetic field measured 15 mm, while that for the electric field was 23 mm long. The transverse electric field was achieved with simple aluminium electrodes, 3 mm far and 5 mm high. The magnetic field (longitudinal or transverse) was obtained by a pair of Helmholtz coils powered by sinusoidal generators. Electric field and transverse magnetic field were oriented according to the horizontal and the first polarizer was oriented at 45 degrees with respect to the direction of the transverse fields. The laser beam after the cuvette was examined by a polarization analyzer oriented at 45 degrees with respect to the first polarizer and finally sent to the photodiode: with this orientation the maximum signal is achievable by modulation due to the Faraday effect (longitudinal magnetic field). The photodiode was a HP 5082-4220 and the spectrum analyzer was an HP 3582A; the signal was sampled at 8000 samples/sec (Figure 3).

Signals analysis software. The analysis with Hamming windowing was performed using home-made analysis software written in Fortran at the Department of Physics (University of Milan). Other tests have been performed using the Sigview® SignalLab software and have exploited Hann and Hamming windowing, with or without Hann smoothing.

Methods

Resonance experiment. We compared the responses of samples of MTs, tubulin and buffer solutions without proteins when subjected to high frequency electromagnetic stimulations.

1. *Tubulin analysis.* The tubulin sample was prepared as previously described (see: *Materials; Tubulin Reconstitution*). 1 ml of tubulin solution was placed in a plastic test tube positioned between the transmitting and receiving antennas. In order to detect possible resonances on specific frequencies, we carried out a frequency scan between 800 MHz and 2500 MHz using a radiofrequencies generator and checking the presence of an absorption resonance, visible by means of a difference in the peak amplitude, with an Avantest TR-3130 spectrum analyzer.

2. *Microtubules analysis*. The MTs sample was prepared as previously described (see: *Materials; Microtubules Reconstitution*). 1 ml of MTs solution has been analyzed as described in the previous section (Tubulin Analysis).
3. *Microtubule buffer without MTs analysis* (see: *Materials; Preparation of Buffer MT*). 1 ml of Buffer MT been analyzed as described in the previous section (Tubulin Analysis).

Birefringence experiment. The tests were performed on solutions of tubulin and MTs, each in its own stabilizing buffer. Then we repeated the tests with tubulin in MTs buffer and with the buffer alone as control.

S1. *Tubulin in T buffer analysis*
    The tubulin sample was prepared resuspending 0.5 mg of lyophilized tubulin in 1 ml of T buffer at 0-4 °C (final tubulin concentration is 0.5 mg/ml).
S2. *Tubulin in MT buffer analysis*
    The tubulin sample was prepared resuspending 0.5 mg of lyophilized tubulin in 1 ml of MT buffer at 0-4 °C (final tubulin concentration is 0.5 mg/ml).
S3. *MT Buffer analysis* (see: Materials; Preparation of MT Buffer). We analyzed 1 ml of MT buffer.
S4. *Microtubules in MT buffer analysis*
    The MT sample was prepared as previously described (see: *Materials; Microtubules Reconstitution*) by using 0.5 mg of lyophilized MTs (final MT concentration is 0.5 mg/ml). We analyzed 1 ml of MT solution.

Each sample solution was submitted to 4 tests:

(a) Transverse electric field (1 volt/cm)
(b) Transverse magnetic field
(c) Longitudinal magnetic field
(d) No field

For each test the value displayed on the polarimeter measures directly the current in the photodiode, expressing the intensity of the laser beam after passing through the cuvette. In presence of a strong scattering, the intensity decreases. The cuvette for the magnetic field was 15 mm long, whereas that for the electric field was 23 mm long. To minimize spurious effects, the windows of the cuvettes are made of coverslip glass about 18 microns thick. The spectrum analyzer window was set to see a width of 50 Hz, within which range the frequencies of the two samples are included, the distilled water 610 Hz reference and the analyzed 632 Hz solution.

We used two cells simultaneously, a first cell was always present with a low intensity longitudinal magnetic field at 610.1Hz frequency and filled with distilled water. This allowed a reference signal in all the various measures on the second cell, excited at a 632 Hz frequency. The choice of almost static fields permitted the highest sensitivity. The frequency (632 Hz) is sufficiently low to exclude dynamic effects. An important point is that for longitudinal magnetic fields a strong Faraday effect is present due to the water contained in the analyzed solution and producing a consistent background noise.

RESULTS AND DISCUSSION

Resonance of Microtubules

In the tubulin analysis of tubulin no significant changes have been detected in the amplitude of the signal received by the spectrum analyzer; while in the MTs analysis we observed at1510 MHz a 0.3 dB lowering of the reference peak (absorption), and between 2060 MHz and 2100 MHz a small lowering of the reference peak (absorption). The Microtubule buffer without MT analysis gave no evidence of absorption.

The outcome of the last analysis is important; the fact that the MT buffer did not cause changes in the reference peak means that the fluctuation found in the test tube with microtubules and MT buffer depends only on the protein assembling in the tubelike structure typical of MTs.

Birefringence Results

Already at an early stage we noticed a strong response to the longitudinal magnetic field of all samples submitted to a frequency of 632 Hz, due at least in large part to the Faraday effect, while without field no reaction peaks were visible.

FFT Analysis of the Acquired Signals

In Table 1 we show the values obtained with different set-ups, normalized by the value of the control sample at 610 Hz [value (632 Hz) / value (610 Hz)] allowing a direct comparison between the analyses. All values have been multiplied by 10^5 factor. The 632 Hz signal is shown normalized for the presence of changes in measurements due to scattering, by comparing this value to the value of the 610 Hz signal of the control sample containing distilled water. The parameter choices were different for each of the four tests shown. Since the signal was sampled at 8000 Hz, the bandwidth per channel is 4000/131072 = 0.003052 Hz/channel and the transformed FFT was performed on 18 bits, or 262,144 points.

The Hann windowing is useful for analyzing transients longer than the length of the window and for general purpose applications. The Hamming windowing is very similar to the previous one; in the time domain it does not come so close to zero near the peak, as the Hann windowing does.

For the Hann window function analysis (WF1) we did not use smoothing; we used instead a 15 pts smoothing (WF2) trying to remove noise without altering the possible relevant data.. The Hamming window function analysis (WF3) had no smooth, while a 5 pts smoothing have been applied in WF4. We did not deepen the analyses on tubulin in tubulin buffer, since the different buffer would affect the possible comparison with the other samples. By comparing the results we observe that there are major differences in values over the third decimal place.

Table 1.

	WF3A	*WF4 D*	*WF1 C*	*WF2BC*
Electric Field (EF)				
S4	0.0267	0.0249	0.0283	0.0238
S2	0.0177	0.0175	0.0197	0.0169
S3	0.0099	0.0089	0.0123	0.0083
S1	0.0025			0.0018
Transverse MagneticFfield (TMF)				
S4	0.0810	0.0781	0.0837	0.0766
S2	0.0996	0.0966	0.1018	0.0946
S3	0.0925	0.0893	0.0953	0.0872
S1	0.0895			0.0849
Longitudinal Magnetic Field (LMF)				
S4	1.828	1.7717	1.8480	1.7320
S2	2.327	2.2544	2.3567	2.2025
S3	2.336	2.2628	2.3654	2.2115
S1	2.311			2.1883
No Field (NF)				
S4	0.00860	0.01069	N P	0.00389
S2	0.00285	0.00135	N P	0.00088
S3	0.00585	0.00353	N P	0.00245
S1	0.00353			0.00112

NP: No Peak in 632 Hz
WF1: Hann window function
WF2: Hann window function (smooth 15 pts)
WF3: Hamming window function
WF4: Hamming window function (smooth 5 pts)

Considering the relationship between the responses of the solutions in each context, we note that for all the analyses the MTs solution gave higher responses. There is a significant difference between the readings of the solution without protein, that gives values about ten times lower than that of the solution with MTs, which suggests a degree of response due to the proteins itself.

The MTs solution always shows higher values than the tubulins solution when crossed by electric field. The tubulins solution always shows larger values than the control solution when an electric field is applied. Tests with buffer alone show values equal to the tests with proteins, this suggests that there was no significant response for MTs and tubulins subjected to transverse magnetic field.

The comparison among the same tests with different windowing and smoothing highlighted the difference in the response of the MTs samples, while for the other solutions the values are virtually identical. The MTs solution has always lower value of both the tubulins solution and the solution alone when crossed by a longitudinal magnetic field. We can also observe that the solution with MTs has always a higher value if compared with the solution with tubulins and the solution alone in absence of electromagnetic field. The value of

the tubulins solution results to be lower than the value of the solution alone in the cases of longitudinal magnetic field and no field.

It should be noted that the various parameterizations lead to small differences in absolute value, but substantially retain the ratio values. The uniformity of the different analysis suggests that these differences are not random or due to noise and, given this correlation, we do not need to evaluate a best choice among possible parameterizations.

Statistical Analysis

Below the statistical analysis is reported to verify possible significances.

With 8000 samples / sec run for 32 seconds, we provided more than 262,000 entries for each set-up. The analysis was performed using the paired t-test. Given the substantial equivalence between parameterizations, the analysis was performed on the significance of data processed with Hamming windowing and Hamming smoothing (5 pts). Comparisons were made on the most interesting portion of data, that includes the frequencies from 600 Hz to 650 Hz.

We compared with Paired T test the data where we had observed different behaviours (Table 2).

Table 2.

	95% CI	T-Value (P-Value)
S4(EF) ; S2(EF)	(-1,1188; -0,9555)	-24,91 (0,000)
S4(EF)* ; S2(EF)*	(0,000733; 0,000873)	22,53 (0,000)
S4(EF) ; S3(EF)	(-2,2282; -2,0130)	-38,66 (0,000)
S4(EF)* ; S3(EF)*	(0,000680; 0,000827)	20,12 (0,000)
S2(EF) ; S3(EF)	(-1,2012; -0,9658)	-18,06 (0,000)
S2(EF)* ; S3(EF)*	(-0,000105; 0,000006)	-1,76 (0,078)
S4(LMF) ; S2(LMF)	(-0,5861; -0,3924)	-9,91 (0,000)
S4(LMF)* ; S2(LMF)*	(0,000570; 0,000724)	16,56 (0,000)
S4(LMF) ; S3(LMF)	(-2,0424; -1,7779)	-28,33 (0,000)
S4(LMF)* ; S3(LMF)*	(0,000427; 0,000593)	12,07 (0,000)
S4(NF) ; S2(NF)	(0,5588; 0,7656)	12,56 (0,000)
S4(NF)* ; S2(NF)*	(0,001982; 0,002171)	43,08 (0,000)
S4(NF) ; S3(NF)	(-0,7297; -0,4794)	-9,47 (0,000)
S4(NF)* ; S3(NF)*	(0,001831; 0,002027)	38,74 (0,000)
S2(NF) ; S3(NF)	(-1,3829; -1,1508)	-21,41 (0,000)
S2(NF)* ; S3(NF)*	(-0,000204; - ,000091)	-5,14 (0,000)

CI: confidence interval for mean difference

T-Value: T-Test of mean difference = 0 (vs not = 0)

* Normalized at 610 Hz

Among all the tests just the Paired T for S2 (Electric Field) normalized at 610 Hz and S3 (Electric Field) normalized at 610 Hz, which compares tubulin in microtubules buffer and buffer without cellular matter, both subjected to electric field, shows a value above the 5% threshold.

All the other comparisons show a good statistical significance, for which the P-Value is always <0.0005, suggesting that the already highlighted differences in the behaviour, allow us to draw some conclusions on the achieved results.

CONCLUSIONS AND FUTURE DEVELOPMENTS

In this work we described the results and analysis of data collected from experiments on MTs and tubulin subjected to electromagnetic stimulations in order to observe possible different behaviours.

In the electromagnetic resonance experiment we identified a difference in the peak amplitude of the solution with MTs at a frequency of 1510 MHz, whereas the solution with tubulin and the control solution did not show any reaction. The lack of response in tubulin and control can be considered a hint that the peculiar structure of microtubules could be the cause of the observed signal.

Considering the nanoscopic size of MTs, the resonance analysis would be more effective if carried out on much higher frequencies (up to 100 GHz), with suitable instrumentation. The presence of a small but sharp resonance effect at a low frequency could be the hint of a much evident effect at higher frequencies.

The analysis of the results of birefringence experiment highlights that the MTs react to electromagnetic fields in a different way than tubulin. In particular, electric field and longitudinal magnetic field show opposite effects in the two types of proteins. Anyway in spite of the effect under electric field is the same as with no field, an unexpected and interesting effect is shown in the case of longitudinal magnetic field. The achieved results, supported by statistical significance, suggest that the tubular structure of MTs might be responsible for the different behaviour in respect to free tubulins. These preliminary positive results encourage us to continue our experimental research. In particular we will carry out a replication of the already performed tests on MTs and tubulins interacting with different ligands. It will be necessary to assess the statistical significance of possible differences in value. The experimental results will be coupled with a three-dimensional simulation of the protein folding binding different ligands, to study the emerging conformational differences. These studies would support hypotheses on the origin of the different biophysical behaviour in relationship with conformational changes. This work aims to deepen the knowledge on the behaviour of MTs and tubulin and to deduce a number of reasonable assumptions on the function of MTs as information or quantum information communication structures.

ACKNOWLEDGMENTS

REFERENCES

[1]   Hyams, J. S. & Lloyd, C. W. (1994). editors. *Microtubules.* Wiley-Liss, New York.

[2]   Postingl, H., Krauhs, E., Little, M. & Kempf, T. (1981). Complete amino acid sequence of α-tubulin from porcine brain. *Proc. Natl. Acad. Sci.*, USA, *78*, 2757–61.

[3]   Krauhs, E., Little, M., Kempf, T., Hofer-Warbinek, R., Ade, W. & Postingl, H. (1981). Complete amino acid sequence of β-tubulin from porcine brain. *Proc. Natl. Acad. Sci. USA.*, *78*, 4156–60.

[4]   Lowe, J. & Amos, L. A. (1998). Crystal structure of the bacterial cell-division protein FtsZ. *Nature.*, *391*, 203–6.

[5]   Nogales, E. (1998). Structure of the αβ-tubulin dimer by electron crystallography. *Letters to nature*, *391*, 192–203.

[6]   Lowe, J., Li, H., Downing, K. H. & Nogales, E. (1998). Refined Structure of αβ-Tubulin at 3.5 A° Resolution. *J. Mol. Biol.*, *313*, 1045–57.

[7]   Amos, L. A. & Schlieper, D. Microtubules and MAPs. *Advances in chemistry*, *Vol. 71,* 257.

[8]   Tuszynski, J. A., Brown, J. A., Crawford, E. & Carpenter, E. J. (2005). Molecular Dynamics Simulations of Tubulin Structure and Calculations of Electrostatic Properties of Microtubules. *Mathematical and computer modeling.*

[9]   Ravelli, R., Gigant, B., Curmi, P. A., Jourdain, I., Lachkar, S., Sobel, A. & Knossow, M. (2004). Insight into tubulin regulation from a complex with colchicine and a stathmin-like domain. *Letters to Nature*, *428*, 198–202.

[10]   Amos, L. A., Amos, W. B. (1991). *Molecules of the Cytoskeleton*, First Edition, MacMillan Press, London.

[11]   Chrétien, D. & Wade, R. H. (1991). New data on the microtubule surface lattice. *Biol Cell.*, *71(1-2)* , 161-74.

[12]   Nogales, E., Whittaker M, Milligan R. A. & Downing, K. H. (1999). *High-Resolution Model of the Microtubule. Cell.* , 96, 79-88.

[13]   Mandelkow, E. M., Mandelkow, E. & Milligan, R. A. (1991). Microtubules dynamics and microtubules caps: a time-resolved cryoelectron microscopy study. *J. Cell Biol.*, *114*, 977–91.

[14]   Binder, L. I. & Rosenbaum, J. L. (1978). The in vitro assembly of flagellar outer doublet tubulin. *J. Cell Biol.*, *79*, 500-15.

[15]   Burton, P. R. & Himes, R. H. (1978). Electron microscope studies of pH effects on assembly of tubulin free of associated proteins. *J. Cell Biol.*, *77(1)*, 120–33.

[16]   Chrétien, D., Metoz, F., Verde, F., Karsenti, E. & Wade, R. H. (1992). Lattice defects in microtubules: Protofilament numbers vary within individual microtubules, *J. Cell Biol.*, *117(5)*, 1031-40.

[17]   Linck, R. W. & Langevin, G. L. (1981). Reassembly of flagellar B (αβ) tubulin into singlet microtubules: consequences for cytoplasmic microtubule structure and assembly. *J. Cell Biol.*, *89*, 323–37.

[18]   Pierson, G. B., Burton, P. R. & Himes, R. H. (1978). Alterations in number of protofilaments in microtubules assembled in vitro. *J. Cell Biol.*, *76*, 223–8.

[19]   Chrétien, D. (2000). Microtubules Switch Occasionally into Unfavorable Configuration During Elongation. *J. Mol. Biol.* , *298*, 663–76.

[20] Savage, C., Hamelin, M., Culotti, J. G., Coulson, A., Albertson, D. G. & Chalfie, M. (1989). MEC-7 is a β-tubulin gene required for the production of 15-protofilament microtubules in Caenorhabditis elegans. *Genes Dev*., *3*, 870–81.

[21] Fukushige, T., Siddiqui, Z. K., Chou, M., Culotti, J. G., Gogonea, C. B., Siddiqui, S. S. & Hamelin, M. (1999). MEC-12, an α-tubulin required for touch sensitivity in C. elegans. *Journal of Cell Science*, *112*, 395–403.

[22] Hameroff, S. R., Penrose, R. Orchestrated reduction of quantum coherence in brain microtubules: A model for consciousness. *Mathematics and Computers in Simulation*, *40*, 453–80.

[23] Hameroff, S. R., Penrose, R. (1996). Conscious events as orchestrated space-time selection. *Journal of Consciousness Studies*, *3*, 36–53.

[24] Tegmark, M. (2000). The importance of quantum decoherence in brain processes. *Phys. Rev. E.*, *61(4)*, 4194–206.

[25] Tegmark, M. (2000). Why the brain is probably not a quantum computer. *Information Science*, *128(3-4)*, 155-79.

[26] Woolf, N. J., Hameroff, S. R. (2001). A quantum approach to visual consciousness. *Trends in Cognitive Science*, *5(11)*, 472–78.

[27] Hagan, S., Hameroff, S. R. & Tuszynski, J. A. (2002). Quantum computation in brain microtubules: Decoherence and biological feasibility. *Physical Review E.*, *65*, 061901–11.

[28] Hameroff, S. R. (2007). The brain is both neurocomputer and quantum computer. *Cognitive Science*, *31*, 1035–45.

[29] Hameroff, S. R. (2007). Orchestrated Reduction of Quantum Coherence in Brain Microtubules. *NeuroQuantology*, *5(1)* , 1–8.

[30] Nanopoulos, D. V. (1995). *Theory of Brain Function, Quantum Mechanics And Superstring*s, http://arxiv.org/abs/hep-ph/9505374.

[31] Nanopoulos, D. V. & Mavromatos, N. (1996). *A Non-Critical String (Liouville) Approach to Brain Microtubules: State Vector Reduction, Memory Coding and Capacity.*, http://arxiv.org/abs/quant-ph/9512021.

[32] Mavromatos, N. (2000). *Cell Microtubules as Cavities: Quantum Coherence and Energy Transfer?* , http://arxiv.org/pdf/quant-ph/0009089.

[33] Mavromatos, N., Mershin, A. & Nanopoulos, D. V. (2002). *QED-Cavity model of microtubules implies dissipationless energy transfer and biological quantum teleportation,* http://arxiv.org/pdf/quant-ph/0204021.

[34] Tuszynski, J., Hameroff, S. R., Satarić, M. V., Trpišová, B. & Nip, M. L. A. (1995). Ferroelectric behavior in microtubule dipole lattices: implications for information processing, signaling and assembly/disassembly. *J. Theor. Biol.*, *174*, 371–80.

[35] Tuszynski, J. A., Trpišová, B., Sept, D. & Satarić, M. V. (1997). The enigma of microtubules and their self-organization behavior in the cytoskeleton. *Biosystems*, *42*, 153-75.

[36] Tuszynski, J. A., Brown, J. A. & Hawrylak, P. (1998). Dielectric Polarization, Electrical Conduction, Information Processing and Quantum Computation in Microtubules. Are They Plausible? Phil. Trans. *The Royal Society. Lond. A.*, 356(1743). 1897–926, 1998.

[37] Faber, J., Portugal, R. & Rosa, L. P. (2006). Information processing in brain microtubules. *Biosystems*, *83(1)*, 1–9.

[38] Del Giudice, E., Doglia, S., Milani, M. & Vitiello, G. (1983). Spontaneous symmetry breakdown and boson condensation in biology. *Phys. Rev. Letts*, *95A*, 508–10.

[39] Del Giudice, E., Doglia, M. & Milani, M. (1982). Self-focusing of Fröhlich waves and cytoskeleton dynamics. *Phys. Letts*, *90A*, 104–06.

[40] Pessa, E. (2007). Phase Transition in Biological Matter. Physics of Emergence and Organization. Licata I, Sakaji A, editors. *World Scientific*; 165-228.

[41] Alfinito, E., Viglione, R. & Vitiello, G. (2001). The decoherence criterio, http://arxiv.org/PS_cache/quant-ph/pdf/0007/0007020v2.pdf.

[42] Vitiello, G. (1995). Dissipation and memory capacity in the quantum brain model. Int. *J. Mod Phys. B*., *9(8)*, 973–89.

[43] Pessa, E. & Vitiello, G. (2004). Quantum noise induced entanglement and chaos in the dissipative quantum model of brain. *Int. J. Mod Phys. B*, *18(6)*, 841–58.

[44] Freeman, W. J. & Vitiello, G. (2006). Nonlinear brain dynamics as macroscopic manifestation of underlying many-body field dynamics, *Phys. of Life Reviews*, *3(2)*, 93–118.

[45] Roche, S., Akkermans, E., Chauvet, O., Hekking, F., Issi, J. P., Martel, R. & Montambaux, G. (2006). Poncharal Ph.. Transport Properties. Understanding Carbon Nanotubes. Loiseau A, Launois P, Petit P, Roche S, Salvetat J-P, editors. *Springer*, *677*, 335–437.

[46] Sapmaz, S., Meyer, C., Beliczynski, P., Jarillo-Herrero, P. & Knowenhoven, L. P. (2006). Excited State Spectroscopy in Carbon Nanotube Double Quantum Dots. *Nano Lett*, *6(7)*, 1350–55.

[47] Pampaloni, F. & Florin, E. L. (2008). Microtubule architecture: inspiration for novel carbon nanotube-based biomimetic materials. *Trends in Biotechnology*, *26(6)*, 302–10,.

[48] Michette, A. G., Mavromatos, N., Powell, K., Holwill, M. & Pfauntsch, S. J. (2004). Nanotubes and microtubules as quantum information carriers. *Proc. SPIE*, *522*, 5581,.

[49] Wang, Y., Kempa, K., Kimball, B., Carlson, J. B., Benham, G., Li, W. Z., Kempa, T., Rybczynski, J., Herczynski, A. & Ren, Z. F. (2004). Receiving and transmitting light-like radio waves: Antenna effect in arrays of aligned carbon nanotubes. *Applied physics letters*, *85(13)*, 2607–9.

[50] Huang, X. R. & Knighton, R. W. (2005). Microtubules Contribute to the Birefringence of the Retinal Nerve Fiber Layer. *Invest Ophthalmol Vis Sci*., *46(12)*, 4588–93, 2005.

[51] Oldenbourg, R., Salmon, E. D. & Tran, P. T. (1998). Birefringence of Single and Bundled Microtubules. *Biophysical Journal*., *74*, 645–54.